Determining coronal bright point size via cross-correlation using multi-wavelength images from AIA/*SDO*

Laurel Farris, R. T. James McAteer
New Mexico State University
laurel07@nmsu.edu

ABSTRACT

Subject headings: Sun: corona-Sun: bright points-

1. Introduction

It is currently thought that after magnetic flux tubes rise from the tachocline of the sun (between the convection and radiative zones) to the photosphere, they are moved across the photosphere by the process of advection to the junctions between supergranules (source?). There they are observed as bright points (BPs). Though they only cover about 1.6 % of the photosphere (Srivastava & Dwivedi (2010)), BPs (together with sunspots) contribute over 90% of the total magnetic flux (Howard & Stenflo (1972)). Over the course of the solar cycle, they can contribute significantly to the global intensity variation of the sun, particularly in the ultraviolet regime (Riethmüller et al. (2014)).

These BPs can be seen in the upper layers of the solar atmosphere in the form of coronal BPs. The cross-sectional area of these BPs is known to increase with height above the photosphere as the density decreases and temperature increases (source?).

Several techniques for determining the size of coronal BPs have been investigated in the literature. Alipour & Safari (2015) developed an algorithm to locate BPs in the corona, using size determined by intensity as part of the criteria for distinguishing BPs from other features, such as top-down views of coronal loops or nanoflares.

The goal for the project discussed in this Letter was to determine size in another way, using the cross-correlation between the pixels in and around the visible area occupied by the BP. The data is described in § 2, the analysis is discussed in § 3, and conclusions are in § 5.

2. Data

This analysis was carried out using multi-wavelength data from AIA/*SDO* spanning one hour on June 1, 2012 from 13:00:00 to 13:59:59, at a cadence of 12 seconds. Each EUV passband corresponds to emission from different transitions of ion species in the corona, each of which takes place at different temperatures, and hence different heights, above the photosphere. The relevant values for each passband are given in table 1.

Wavelength [Å]	Temperature [K]
94	$10^{6.8}$
131	$10^{5.6}, 10^{7.0}$
171	$10^{5.8}$
193	$10^{6.2}, 10^{7.3}$
211	$10^{6.3}$
304	$10^{4.7}$
335	$10^{6.4}$

Table 1: Characteristic temperatures corresponding to the wavelengths observed in emission in the solar corona (taken from Lemen et al. (2012)).

A single BP from a coronal hole located in the full disk was selected for analysis. Grayscale images showing this BP in each passband are shown in figure 1.

3. Analysis

The intensity of each BP as a function of radius gives a visual estimate of the size of the BP. For comparison, the intensity of the first image in each passband is plotted as a function of radial distance from the center pixel in figures 6 and 7.

For this project, the size was estimated by running a cross-correlation between a pixel roughly in the center of the BP and the remaining pixels over the 100×100 pixel^2 area through the full hour long time series. The central pixel was arbitrarily determined by locating the brightest pixel in the center of the BP from the first image in the time series. The cross-correlation analysis helps to determine what parts of the feature are moving together as a single physical structure.

4. Results

Images illustrating the highest cross-correlation value of each pixel and the timelag corresponding to that correlation value are shown in figures 2 and 3. The correlation was cut off at 0.5 and rescaled to obtain a better illustration of the structure of the BP. These images are shown in figures 4 and 5.

As Alipour & Safari (2015) noted, the BP structure is most evident for the 131Å, 193Å, and 211Å images.

The 211Å data is particularly notable as it shows strong correlation values at two points to the right of where the BP appears visually in figure 1. A movie showing all images from this wavelength (**?**) revealed a flash of emission around the ?th image.

5. Conclusion

REFERENCES

Alipour, N., & Safari, H. 2015, ApJ, 807, 175

Howard, R., & Stenflo, J. O. 1972, Sol. Phys., 22, 402

Lemen, J. R., Title, A. M., Akin, D. J., et al. 2012, Sol. Phys., 275, 17

Riethmüller, T. L., Solanki, S. K., Berdyugina, S. V., et al. 2014, A&A, 568, A13

Srivastava, A. K., & Dwivedi, B. N. 2010, MNRAS, 405, 2317

This 2-column preprint was prepared with the AAS LaTeX macros v5.2.

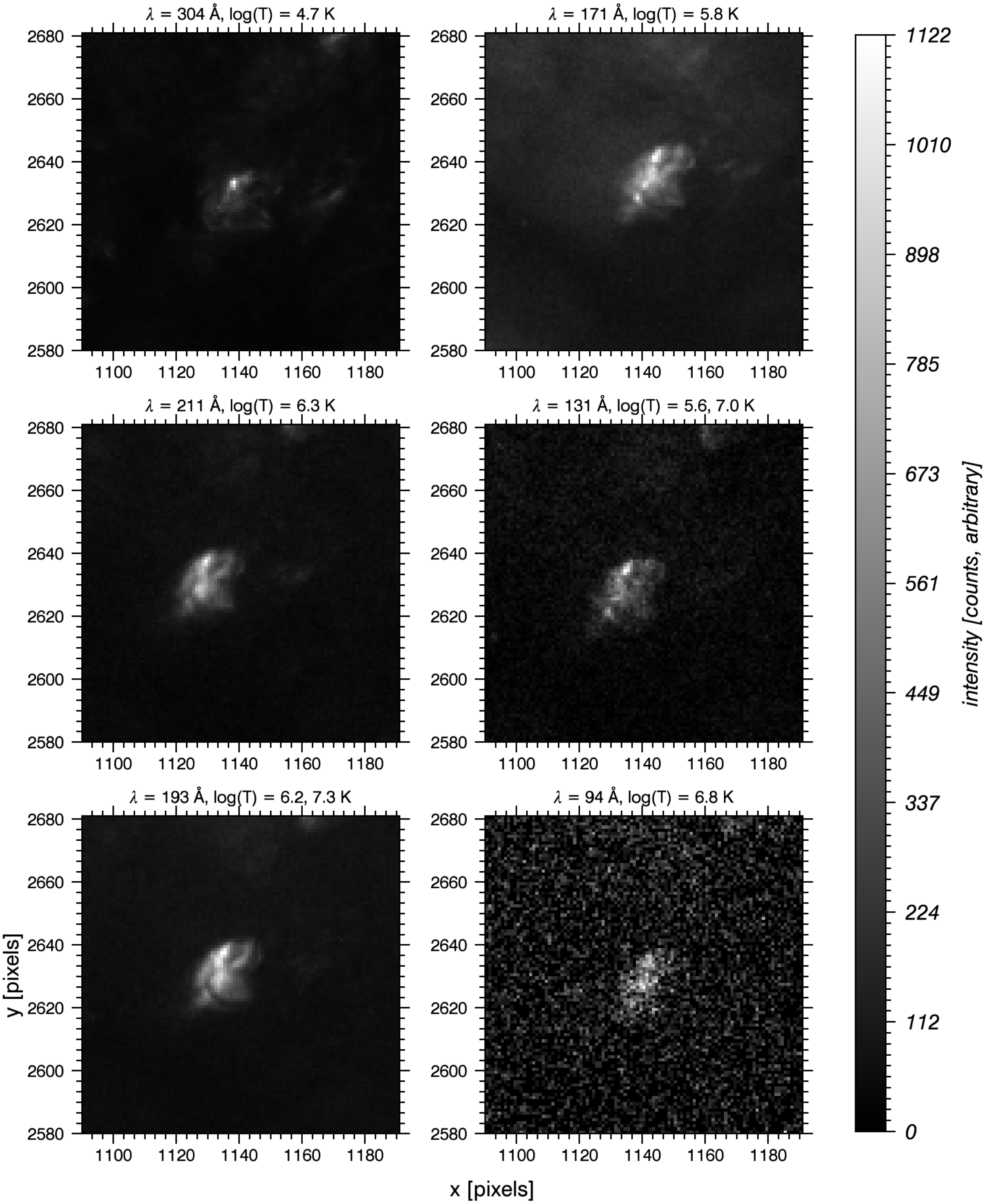

Fig. 1.— Images of the BP in six different AIA wavelengths.

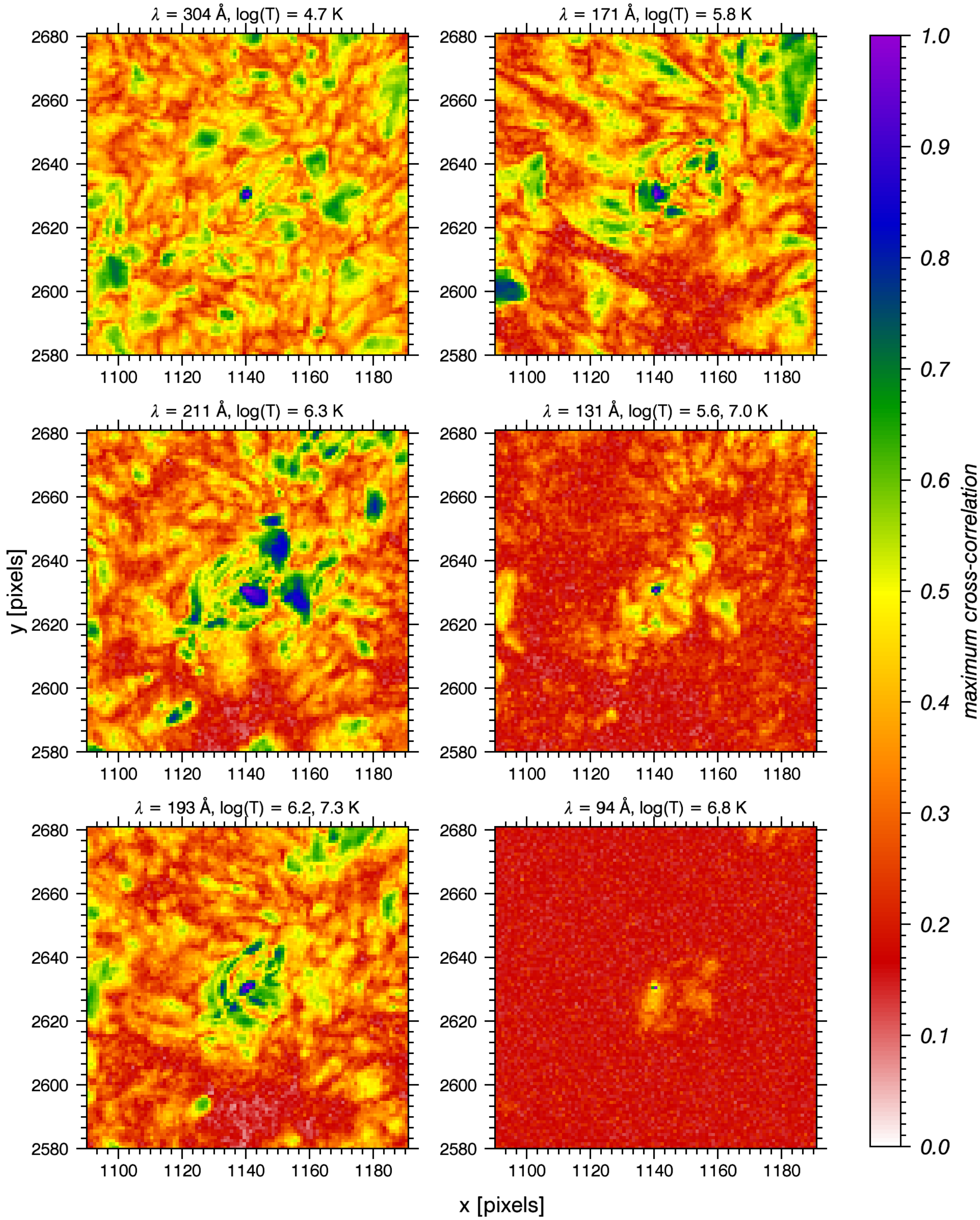

Fig. 2.— Images showing the highest cross-correlation value for each pixel.

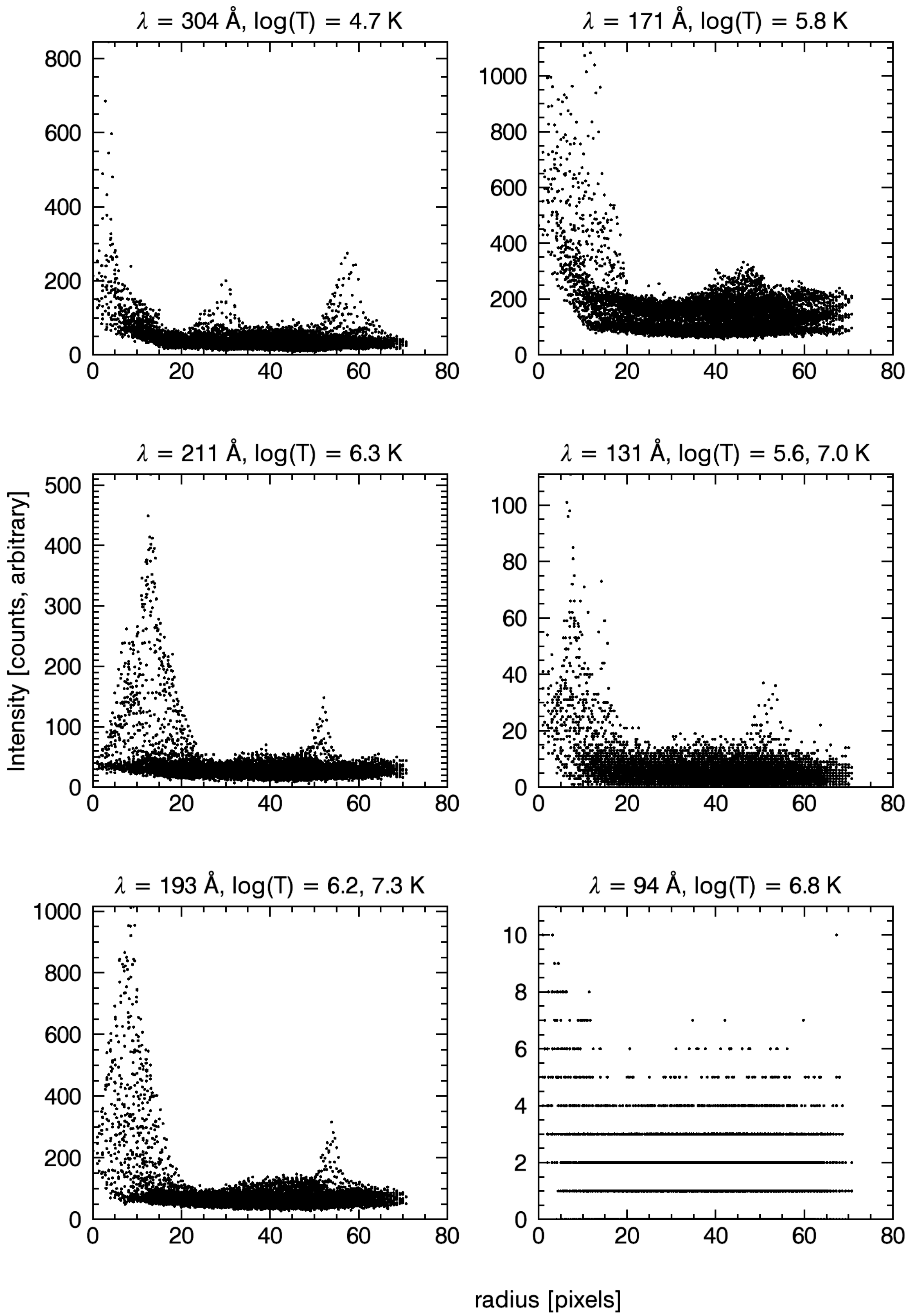

Fig. 3.— Images showing the timelag corresponding to the correlation values illustrated in figure 2. (This is not the correct image; I accidently overwrote the correct one, but can't re-create it because IDL is giving me syntax errors on my function keywords for no apparent reason.)

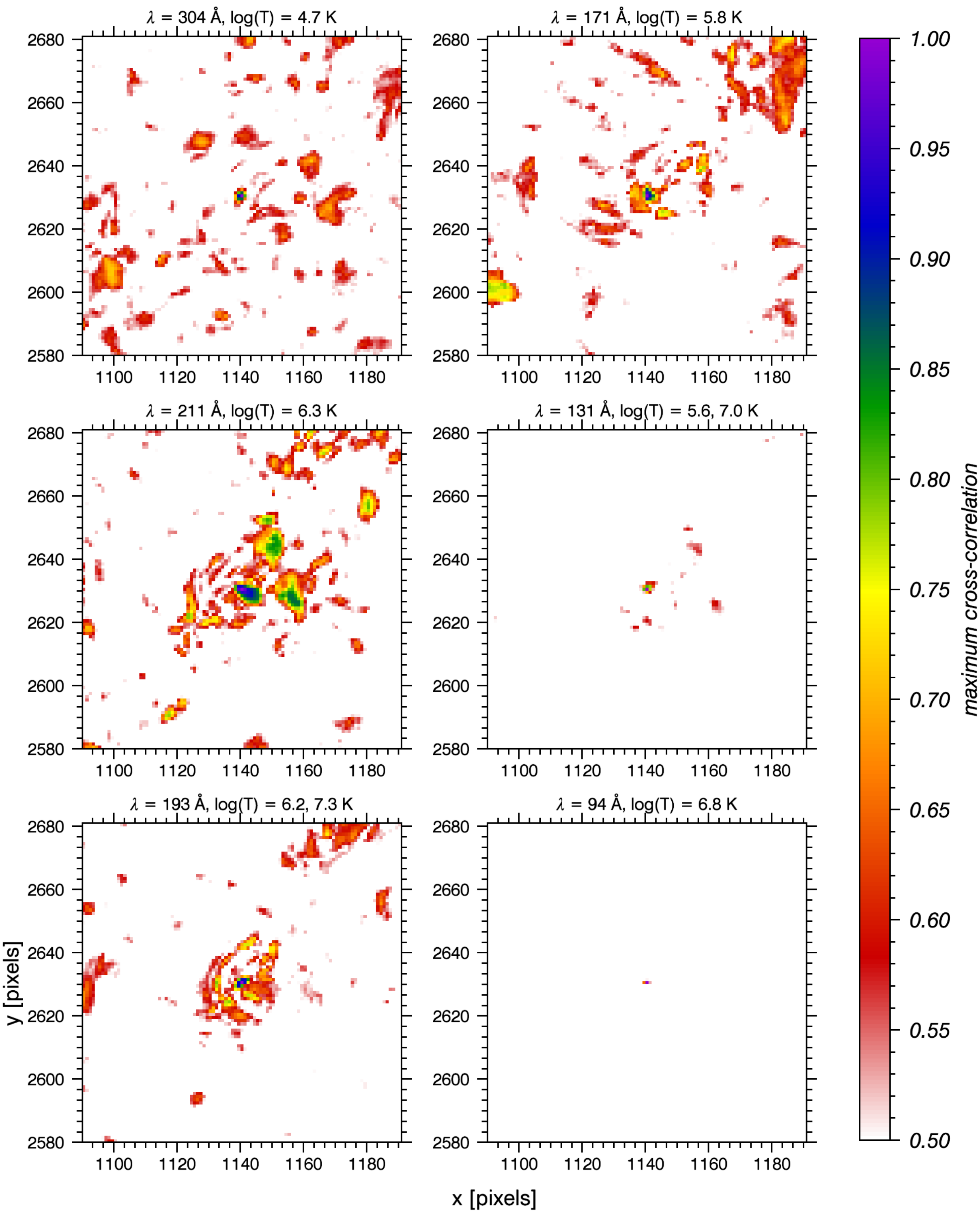

Fig. 4.— Cross-correlation images scaled to show only values higher than 0.5.

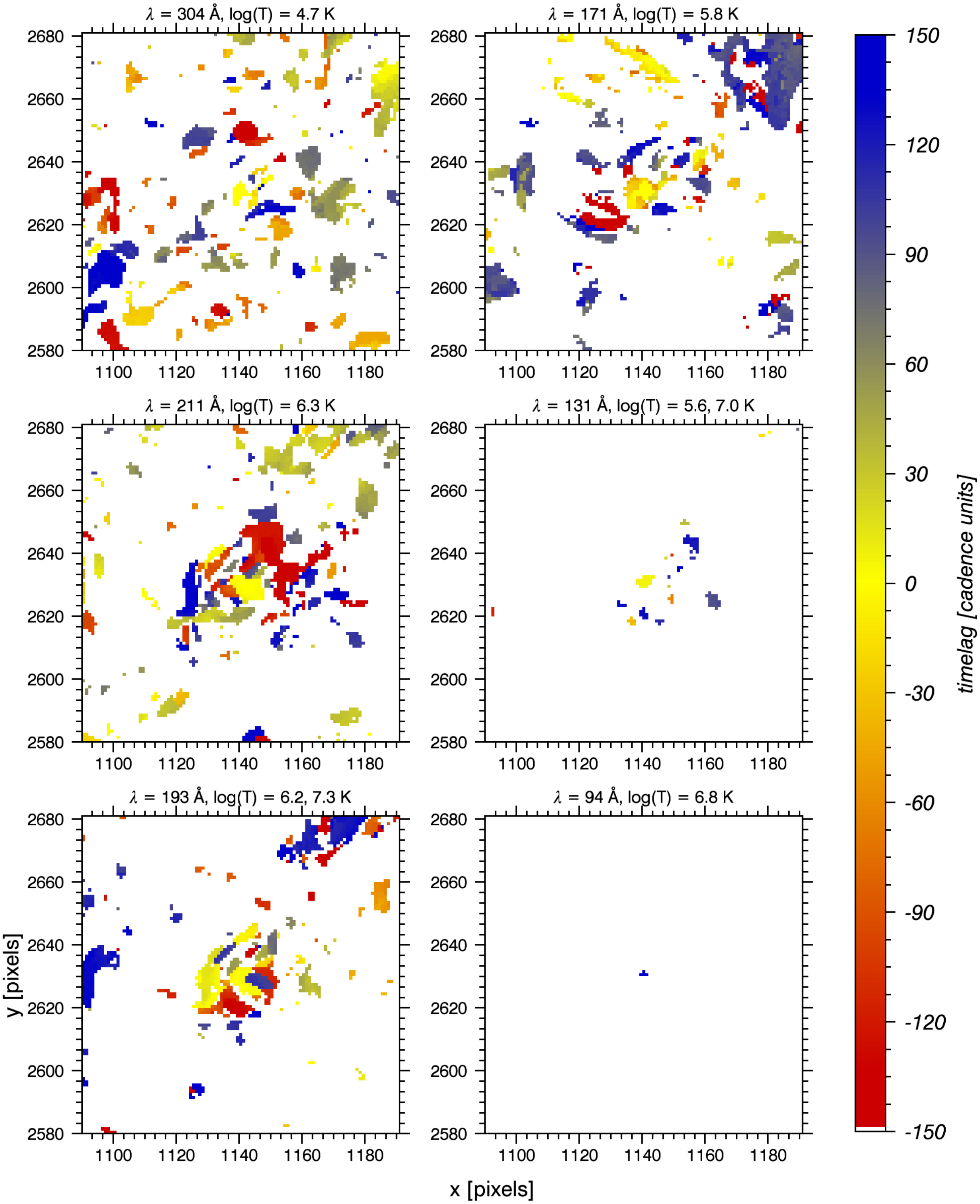

Fig. 5.— Timelag corresponding to the cross-correlation values higher than 0.5.

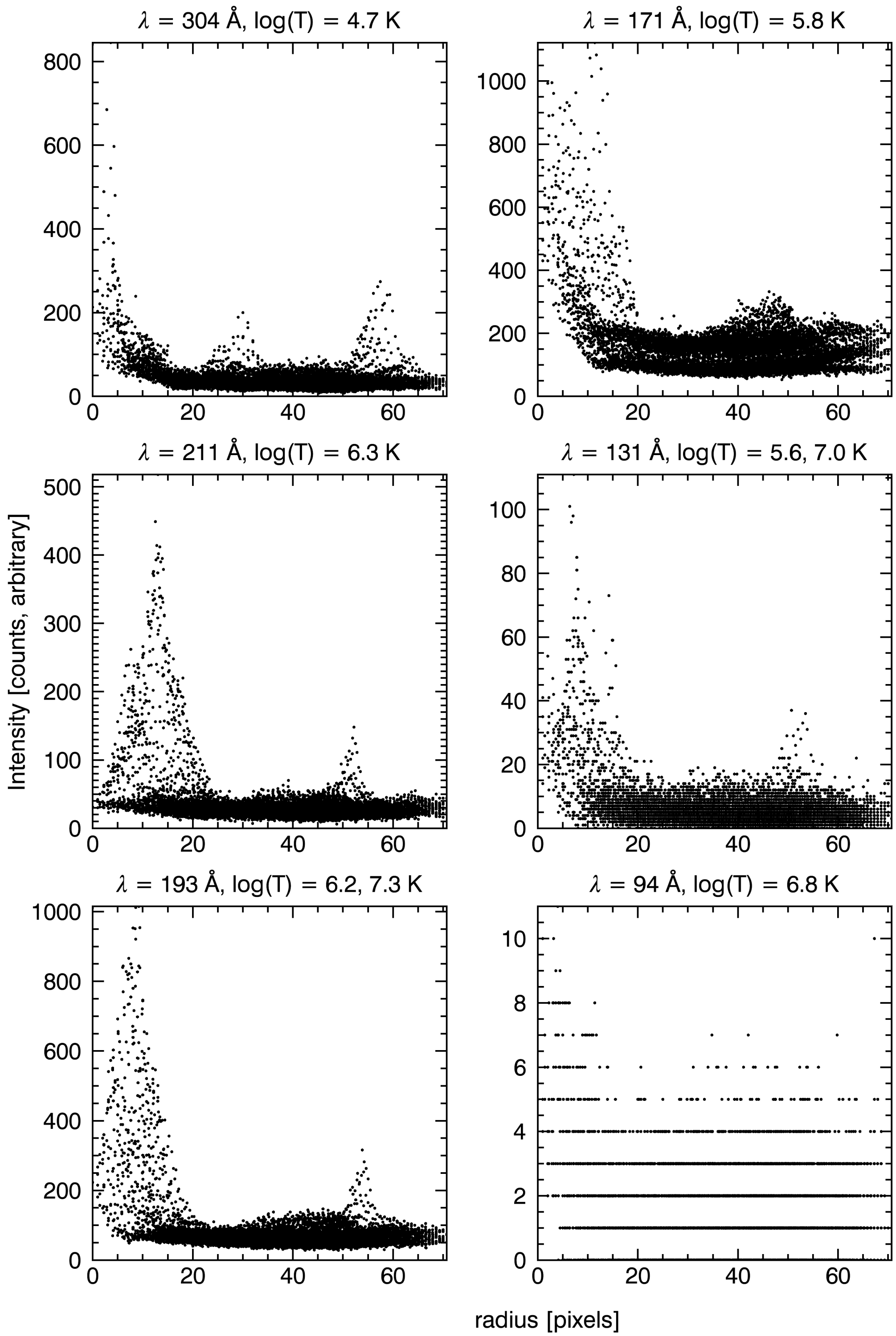

Fig. 6.— Intensity of each pixel is plotted as a function of radius for each passband.

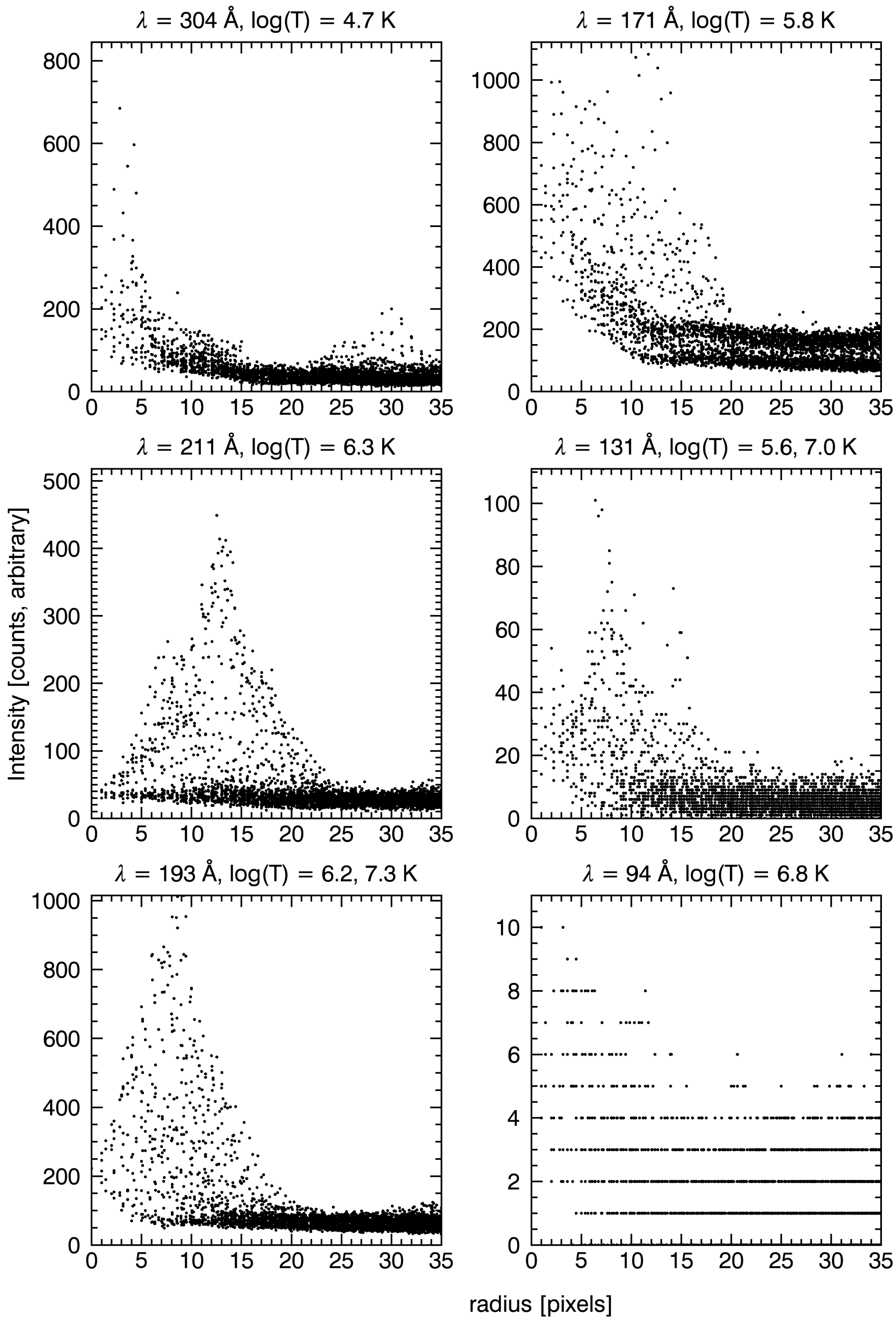

Fig. 7.— Same as figure 6, but with half the radius range cut off to better view the values around the main BP.

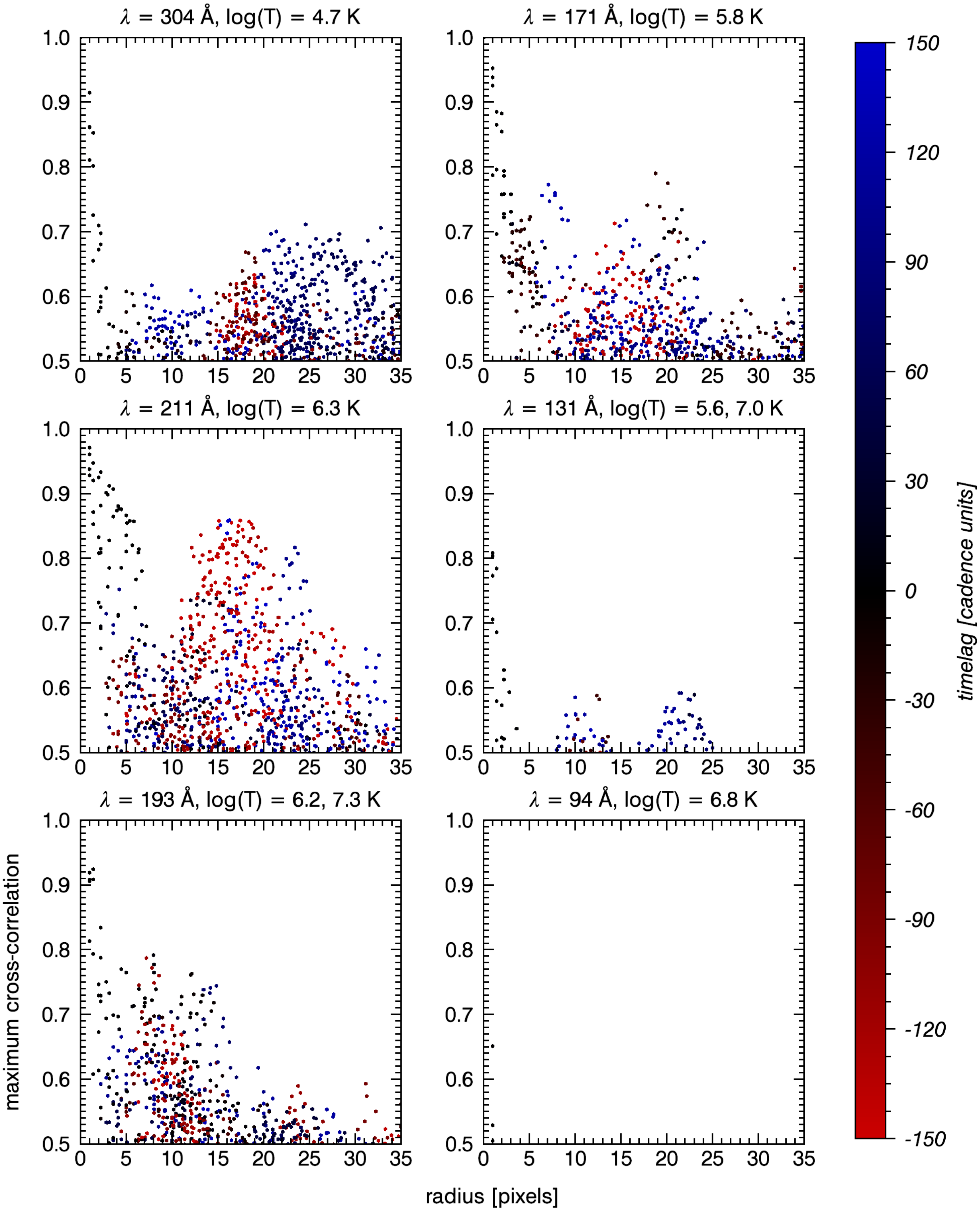

Fig. 8.— The highest cross-correlation value of each pixel is plotted as a function of its distance from the center pixel. The color indicates the timelag corresponding to the maximum cross-correlation for that pixel.

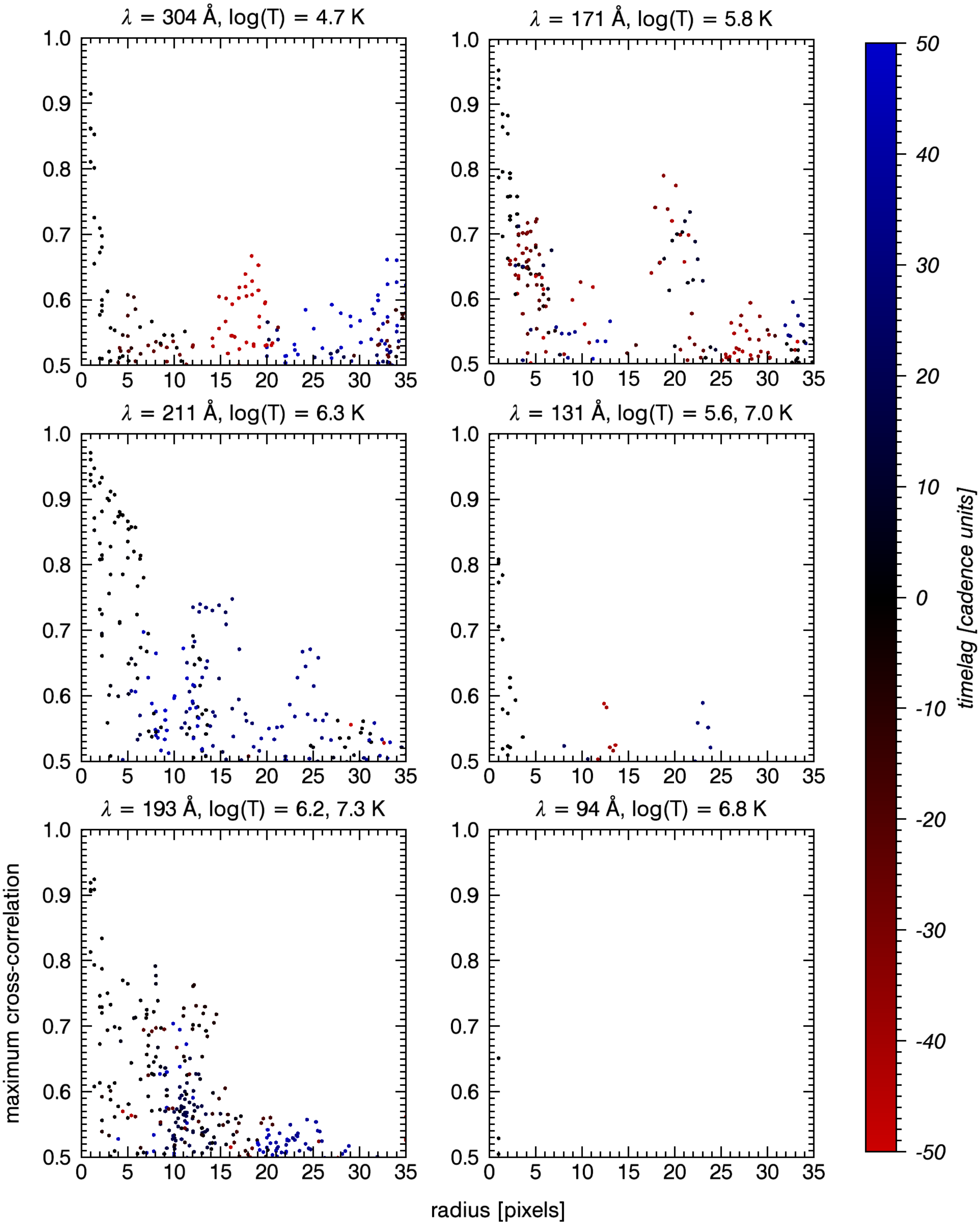

Fig. 9.— Same as figure 8, but with two thirds of the timelag cut out at both ends.